This article has been accepted for publication in a future issue of this journal, but has not been fully edited. Content may change prior to final publication. Citation information: DOI 10.1109/TIE.2014.2362495, IEEE Transactions on Industrial Electronics

A Novel Integrated Power Quality Controller for Microgrid

Dayi Li, *Member, IEEE*, Z. Q. Zhu, *Fellow, IEEE*

***Abstract*—A novel variable reactor based on magnetic flux control is proposed in the paper. The system configuration of the novel variable reactor is presented, whilst its operational principle and dynamic performance are analyzed. Based on the developed variable reactor, a novel integrated power quality controller suitable for microgrid is proposed, which can cater for the peculiar requirements of microgrid power quality, such as the harmonic high penetration, frequent voltage fluctuation and overcurrent phenomenon, bidirectional power flow and small capacity etc. For the fundamental, the equivalent impedance of the primary winding is a variable reactor or capacitor. For the nth order harmonic, the equivalent impedance is very high impedance and acts as a "harmonic isolator". The system control strategy is also analyzed in detail. A set of three-phase integrated power quality controller has been constructed. The experimental test results verify the validity of the novel variable reactor and the integrated power quality controller.**

***Index Terms*—Microgrid, Overcurrent, Power Flow, Power Quality, Transformer, Variable Reactor**

I. INTRODUCTION

Distributed power generation has been emerged as a promising option to meet the growing customer needs for electric power with an emphasis on reliability and environmentally friendly renewable energy. In this context, in order to maximize the operational efficiency of the distributed energy resources (DER) and take full advantage of distributed power generation, as an effective means of integrating DERs into the traditional power grid, microgrid is presented, which can enhance the local customer power supply reliability and system performance, reduce the impact on large power grid and minimize the system losses. Microgrid has good environmental and economical benefits and also has attracted more and more attentions of power researchers [1]-[6]. Whereas the power quality problem of microgrid is much more serious than that of the traditional grid because of the intermittent and random of DERs, the high penetration between conventional grid and microgrid, the diversity of DERs, load, energy conversion unit, storage and operating state. Microgrid power quality has the following unique features compared to the conventional power grid [7]-[16].

1) Background harmonic of DERs and harmonic high penetration are more serious than the traditional grid [17]-[22]. Traditional grid has less system background harmonic and the harmonic is mainly from the nonlinear load. However, in microgrid, besides the nonlinear load, DERs and energy storage converter system access to microgrid may also generate harmonics.

2) Bidirectional power flow control is much more challengeable [23]-[27]. Traditional distribution network is with the features of "passive network" and "one-way power flow", whereas the microgrid is with the features of "active network" and "bidirectional power flow".

3) Voltage fluctuation and sag often happen in microgrid [28]-[31]. In microgrid, except the voltage fluctuation and sags from the load change, most kinds of DERs, which are intermittent and random, will cause significant voltage fluctuations in distribution network.

4) The overvoltage and overcurrent phenomena is more frequent [32]-[34]. In general, microgrid is comparatively small in capacity and the effect of load fluctuation on microgrid is more than that of the traditional power grid. Beside this, control mode switching of many converters connecting in parallel to busbar and the seamless state transition may produce overvoltage and overcurrent.

So far, relevant researches on microgrid power quality controllers can be sorted into two types: unifunctional controllers and multifunctional controllers. Unifunctional power quality controllers aim at a specific power quality issue in microgrid. Harmonic mitigation is mainly investigated in [20]-[22]. Power flow control of microgrid is mostly analyzed in [25]-[28]. Voltage fluctuation is primarily concerned in [27]-[30]. The overvoltage and overcurrent issue is main concern in [33]-[34]. Multifunctional power quality controllers generally combine the power quality controller with the grid-interfacing converter through special control scheme [18], [35] or topology [31]. However, these multifunctional power quality controllers do not take into account all of the abovementioned features of microgrid.

To date there is less research on integrated power quality controller (IPQC) particularly suitable for microgrid with

Manuscript received March 30, 2014; revised March 31, 2014 and July 18, 2014; accepted September 6, 2014.

This work was supported by the National Natural Science Foundation of China under projects 51477060 and 51277081.

Dayi Li is with the State Key Laboratory of Advanced Electromagnetic Engineering and Technology, Huazhong University of Science and Technology, Wuhan 430074 China (email: ldy@mail.hust.edu.cn).

Z. Q. Zhu is with the Department of Electronic and Electrical Engineering, The University of Sheffield, Sheffield, S1 3JD, U.K. (email: Z.Q.Zhu@sheffield.ac.uk).

This article has been accepted for publication in a future issue of this journal, but has not been fully edited. Content may change prior to final publication. Citation information: DOI 10.1109/TIE.2014.2362495, IEEE Transactions on Industrial Electronics

abovementioned features. Also, the microgrid capacity is comparatively small and it is not cost effective to install various types of power quality controller. In order to solve these problems, a novel variable reactor based on magnetic flux control is firstly proposed. In order to cater for the peculiar requirements of microgrid of harmonic high penetration, frequent voltage fluctuation and overcurrent phenomenon, bidirectional power flow and small capacity, a novel integrated power quality controller suitable for microgrid is proposed based on the novel variable reactor. The integrated power quality controller is characterized by mitigating the harmonic penetration, controlling the bidirectional power flow, limiting the fault current and compensating the voltage fluctuation and being a variable reactor. Finally, experimental results are provided to validate the analyses.

II. Principle of Variable Reactor

A. System Configuration

Fig.1 shows the single-phase system configuration of the novel variable reactor based on magnetic flux control (MFC). Suppose the turns of primary and secondary winding of the transformer are N_1 and N_2, respectively. The turns ratio is represented by $k=N_1/N_2$. A transformer with air gap is selected and its primary winding AX can be connected in series or parallel with power utility. The secondary winding ax is not connected with a normal load but a voltage-sourced inverter. The voltages of the primary and secondary winding are u_1 and u_2, respectively. The primary winding current i_1 of the transformer is detected and functions as the reference signal i_{ref}. h is the gain of the current sensor. U_{d} is the voltage of DC side of the inverter. C_{d} stands for the capacitance of the DC capacitor. α is a controllable parameter, which will be explained later. The voltage-sourced inverter and current control are applied to yield a controlled current i_2, which has the same frequency as i_1. i_2 is inversely in phase injected to the secondary winding ax.

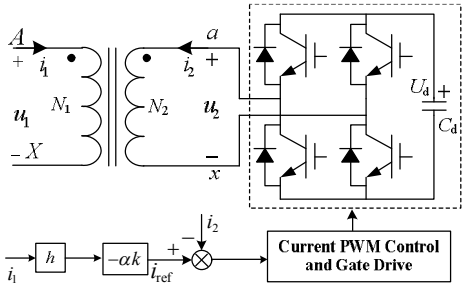

Fig.1 System configuration of novel variable reactor

B. Equivalent T-circuit of Transformer

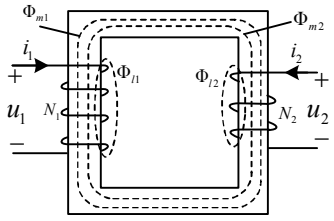

Fig.2 Magnetically coupled circuit of transformer

The magnetically coupled circuit of the transformer is central to the operation of the novel variable reactor, which is shown in Fig.2. The flow of currents in the two windings produces magneto-motive forces (mmf) which in turn set up the fluxes.

The total flux linking each winding may be expressed as

$$\Phi_1 = \Phi_{l1} + \Phi_{m1} + \Phi_{m2} = \Phi_{l1} + \Phi_m \tag{1}$$

$$\Phi_2 = \Phi_{l2} + \Phi_{m2} + \Phi_{m1} = \Phi_{l2} + \Phi_m \tag{2}$$

Herein Φ_{l1} and Φ_{l2} are the leakage fluxes of primary and secondary windings. Φ_{m1} is the magnetizing flux produced by primary winding and it links all turns of primary and secondary windings. Φ_{m2} is the magnetizing flux produced by secondary winding and it links all turns of primary and secondary windings. Φ_m denotes the resultant mutual flux.

The voltage equations of the transformer can be expressed as [36]-[37]

$$u_1 = r_1 i_1 + d\lambda_1 / dt \tag{3}$$

$$u_2 = r_2 i_2 + d\lambda_2 / dt \tag{4}$$

where r_1 and r_2 are the resistances of primary and secondary winding, respectively. λ_1 and λ_2 are flux linkages related to primary and secondary windings, respectively. If saturation is neglected and the system is linear, the following equations can be achieved

$$\lambda_1 = L_{l1} i_1 + L_{m1}(i_1 + \frac{N_2}{N_1} i_2) \tag{5}$$

$$\lambda_2 = L_{l2} i_2 + L_{m2}(\frac{N_1}{N_2} i_1 + i_2) \tag{6}$$

Herein, L_{l1} and L_{l2} are the leakage inductances of primary and secondary winding, respectively. L_{m1} and L_{m2} are the magnetizing inductances of the primary and secondary windings, respectively. $L_{m1}/N_1^2 = L_{m2}/N_2^2$. According to [36]-[37], when the quantities of the secondary winding are referred to the primary winding, (3) and (4) become

$$u_1 = r_1 i_1 + L_{l1}\frac{di_1}{dt} + L_{m1}\frac{d}{dt}(i_1 + i_2') \tag{7}$$

$$u_2' = r_2' i_2' + L_{l2}'\frac{di_2'}{dt} + L_{m1}\frac{d}{dt}(i_1 + i_2') \tag{8}$$

Here the prime denotes referred quantities of secondary winding to primary winding. Equations (7) and (8) can be expressed as the following equation in phasor form

$$U_1 = r_1 I_1 + j\omega L_{l1} I_1 + j\omega L_{m1}(I_1 + I_2') \tag{9}$$

$$U_2' = r_2' I_2' + j\omega L_{l2}' I_2' + j\omega L_{m1}(I_1 + I_2') \tag{10}$$

The voltage equations in (9) and (10) with the common L_{m1} suggest the equivalent T-circuit shown in Fig. 3 for the two-winding transformer.

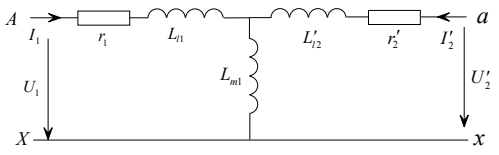

Fig.3 Equivalent T-circuit of transformer

This article has been accepted for publication in a future issue of this journal, but has not been fully edited. Content may change prior to final publication. Citation information: DOI 10.1109/TIE.2014.2362495, IEEE Transactions on Industrial Electronics

Note that in some equivalent T-circuit of the transformer, a core-loss resistance r_m, which accounts for the core-loss due to the resultant mutual flux, is connected in parallel or series with the magnetizing inductance L_{m1} (in the later analysis, a series core-loss resistance r_m is taken into account in the equivalent T-circuit of transformer).

Let $Z_1=r_1+j\omega L_{l1}$, which is the leakage impedance of the winding. $Z'_2=r'_2+j\omega L'_{l2}$, which is the leakage impedance of the secondary winding *ax* referred to primary winding. $Z_m=r_m+j\omega L_{m1}$, which is the magnetizing impedance of the transformer. Here, ω is the fundamental angular frequency. And then (9) and (10) become

$$U_1 = Z_1 I_1 + Z_m (I_1 + I'_2) \tag{11}$$

$$U'_2 = Z'_2 I'_2 + Z_m (I_1 + I'_2) \tag{12}$$

C. Principle of Variable Reactor

In Fig.1, the primary winding current is detected and functions as the reference signal, and the voltage-sourced inverter is applied to track the reference signal so as to yield a controlled current i_2. When controlled current i_2 and the primary current i_1 satisfy

$$I'_2 = -\alpha I_1 \text{ (i. e., } I_2 = -\alpha k I_1) \tag{13}$$

Herein, α is a controllable parameter.

The transformer is double side energized and then the following equations can be obtained.

$$U_1 = Z_1 I_1 + (1-\alpha) Z_m I_1 \tag{14}$$

$$U'_2 = Z'_2 I'_2 + (1-1/\alpha) Z_m I'_2 \tag{15}$$

In terms of (14), from the terminals *AX*, the equivalent impedance of the transformer can be obtained.

$$Z_{AX} = U_1 / I_1 = Z_1 + (1-\alpha) Z_m \tag{16}$$

In terms of (16), the equivalent impedance of the primary winding of the transformer is a function of the controllable parameter α. When α is adjusted, the primary winding exhibits consecutively adjustable impedance.

The equation (16) can also be achieved in terms of the resultant magneto-motive forces of the two windings acting around the same path of the core. When a controlled current i_2 produced by a voltage-sourced inverter is injected into the secondary winding of the transformer and $i_2 = -\alpha k i_1$, the resultant mmf is $N_1 I_1 + N_2 I_2 = (1-\alpha) N_1 I_1$. Then, the resultant flux set up by mmf of the two windings is $(1-\alpha)\ \Phi_m$. And then, the induced voltage produced by the resultant flux can be expressed in phasor form as

$$E_1 = (1-\alpha)\, j\omega L_m I \tag{17}$$

The primary voltage equation can be achieved as (14).

In terms of (16), the relation between the equivalent impedance of the primary winding and the parameter α is shown in TABLE I.

The variable reactor features hardly producing harmonics, simple control scenario and with consecutive adjustable impedance. Many FACTS devices can be implemented in terms of the novel principle [38]. the variable reactor can be used in UPFC to change the line impedance between the sending and receiving ends so as to control the power flow; it can also substitute the thyristor controlled reactor of TCSC, however, the proposed variable reactor does not produce any harmonics; FCL can also be implemented in terms of the novel principle of the variable reactor. Reactive power compensation all can be realized by the novel variable reactor. Also, it has been successfully applied the hybrid series active power filter based on fundamental magnetic flux compensation.

TABLE I
EQUIVALENT IMPEDANCE OF PRIMARY WINDING OF TRANSFORMER

α	The equivalent impedance of terminal *AX*	Impedance characteristic
$\alpha < 0$	$Z_{AX} > Z_1 + Z_m$	resistive and inductive
$\alpha = 0$	$Z_{AX} = Z_1 + Z_m$	
$0 < \alpha < 1$	$Z_1 < Z_{AX} < Z_1 + Z_m$	
$\alpha = 1$	$Z_{AX} = Z_1$	
$1 < \alpha < 1 + Z_1 / Z_m$	$Z_1 < Z_{AX} < 0$	
$\alpha = 1 + Z_1 / Z_m$	$Z_{AX} = 0$	0
$\alpha > 1 + Z_1 / Z_m$	$Z_{AX} < 0$	resistive and capacitive

D. Dynamic Analysis of Variable Reactor

One of the key techniques of the novel variable reactor based on the magnetic flux control is current control. Nowadays the widely used current control technique includes the hysteresis current control, the ramp comparison current control and predictive and deadbeat control [15]. In the digital control system based on DSP, the most widely used current control is the ramp comparison current control with PI controller. In this case, the system block diagram of variable reactor system is shown in Fig. 4. Herein, h is gain of current sensor, the combined transfer function of the sample and delay is represented as $G_{di}(s)=1/(1+sT_{di})$, transfer function of the voltage-sourced inverter is denoted as $G_{PWM}(s)=K_{PWM}/(1+sT_{PWM})$. The transfer function of the PI controller is denoted as $G_{PI}(s)=k_i(1+sT_i)/sT_i$. The system admittance transfer function can be derived as (18) ((18) is below Fig. 4), which means the overall system is a 5 order system. The current control component is in dash-dotted frame shown in Fig.4. In order to improve the system anti-interference performance in low-frequency band, a feed forward element is designed in the block diagram of current control component, which is shown in Fig.5. In this case, the block diagram of current control component becomes Fig. 6. The open-loop transfer function of current control block in Fig.6 is

$$G_{open}(s) = \frac{hk_i(1+sT_i)K_{PWM}}{(1+T_{di}s)sT_i(1+T_{PWM}s)(r_2+r_m+sl_{2\sigma}+sl_m)} \tag{19}$$

Let $T_i = (l_{2\sigma}+l_m)/(r_2+r_m)$ and $T_{PWM} \approx 0.5T_{di}$, When combining the two elements with little time delay, (16) becomes

$$G_{open}(s) = \frac{hK_{PWM}k_i/(r_2+r_m)}{(1+1.5T_{di}s)sT_i} \tag{20}$$

Here, when $k_i=T_i\ (r_2+r_m)/(3T_{di}K_{PWM}h)$, the current control system performance will be approximately optimum [39].

E. DC-link Voltage Control of Variable Reactor

There must be some losses when the novel variable reactor

This article has been accepted for publication in a future issue of this journal, but has not been fully edited. Content may change prior to final publication. Citation information: DOI 10.1109/TIE.2014.2362495, IEEE Transactions on Industrial Electronics

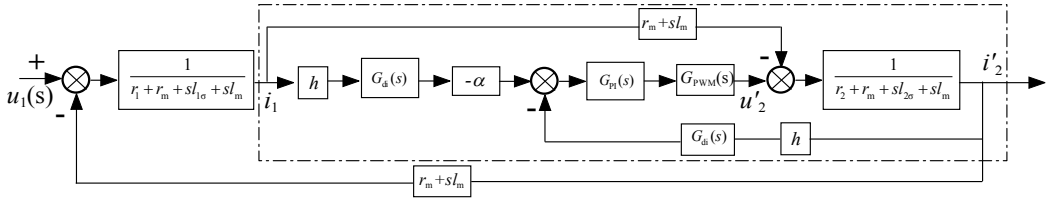

Fig. 4 System block diagram of variable reactor

$$G_Y(s)=i_1(s)/u_1(s)= \frac{hk_i(1+T_is)K_{PWM}+(r_2+r_m+sl_{2\sigma}+sl_m)(1+T_{di}s)sT_i(1+T_{PWM}s)}{hk_i(1+T_is)K_{PWM}[r_1+r_m+sl_{1\sigma}+sl_m-\alpha(r_m+sl_m)]+[(r_1+sl_{1\sigma})(r_2+sl_{2\sigma})+(r_m+sl_m)(r_1+r_2+sl_{1\sigma}+sl_{2\sigma})](1+T_{di}s)sT_i(1+T_{PWM}s)} \quad (18)$$

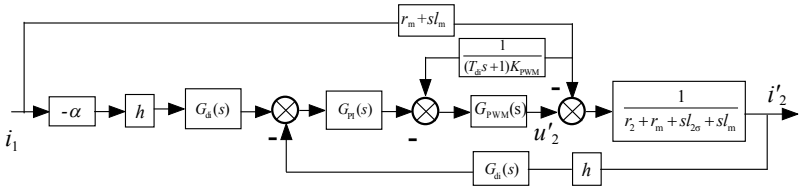

Fig. 5 Block diagram of current control with feed forward

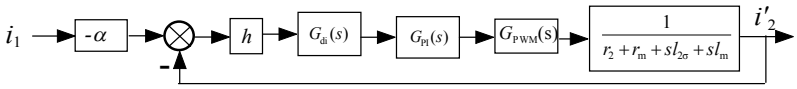

Fig. 6 Block diagram of current control

system with inverter operates normally and the inverter will absorb active power to maintain the DC voltage constant. Fig.7 shows the dc-link voltage control schematic diagram of the variable reactor system. Herein, U_d^* and U_d represent the inverter DC reference and practical voltage, respectively. An active current reference i_p is added to the reference signal i_{refl} to achieve a new reference signal i_{ref2}. A dc-link voltage PI controller is applied to make inverter DC practical voltage U_d to follow the DC reference voltage U_d^*. The output of voltage PI controller is multiplied by phase-lock-loop output of u_2 to yield the active current reference i_p.

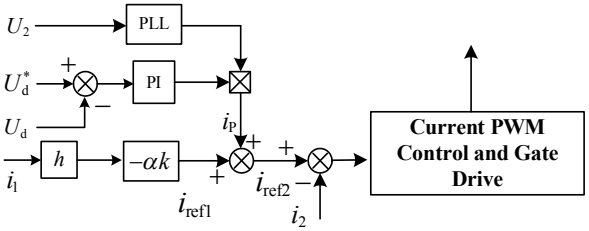

Fig.7 DC-link voltage control schematic diagram

III. PRINCIPLE OF THE INTEGRATED POWER QUALITY CONTROLLER

A. System Configuration

The novel integrated power quality controller can be installed in series and parallel in microgrid or point of common couplings (PCC). For simplicity, the IPQC is installed in PCC. Fig.8 shows the three-phase detailed system configuration of the integrated power quality controller with transformer and inverter. U_s and L_s represent the source voltage and impedance of conventional power supply, respectively. The passive filters, which have the function of absorbing the harmonics, are shunted in both sides. The primary winding of a transformer is inserted in series between the conventional power utility and the microgrid, while the secondary winding is connected with a voltage-source PWM converter. U_d is the voltage of DC side of the inverter. The microgrid contains a harmonic load, a Photovoltaic cell system, battery storage system and a normal load. The proposed integrated power quality controller has the following functions.

B. Power Flow Control

When the power flow control and fault current limiter is concerned, only the fundamental is taken into account.

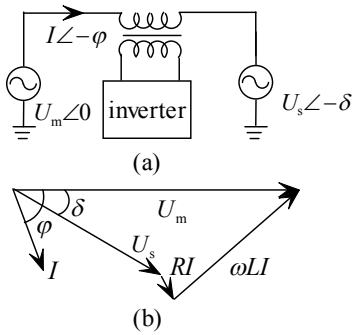

Fig. 9 Power flow control principle and its vector diagram

In terms of the above analysis, the primary winding exhibits adjustable impedance $Z_1 + (1-\alpha)Z_m$. With the change of coefficient α, the equivalent impedance of the primary winding can be achieved, which is shown in TABLE I. Therefore, when the primary winding is connected in series in circuit, it can be applied to control the power flow between the conventional power utility and the microgrid or the internal power flow of microgrid. The schematic diagram of power flow control is

This article has been accepted for publication in a future issue of this journal, but has not been fully edited. Content may change prior to final publication. Citation information: DOI 10.1109/TIE.2014.2362495, IEEE Transactions on Industrial Electronics

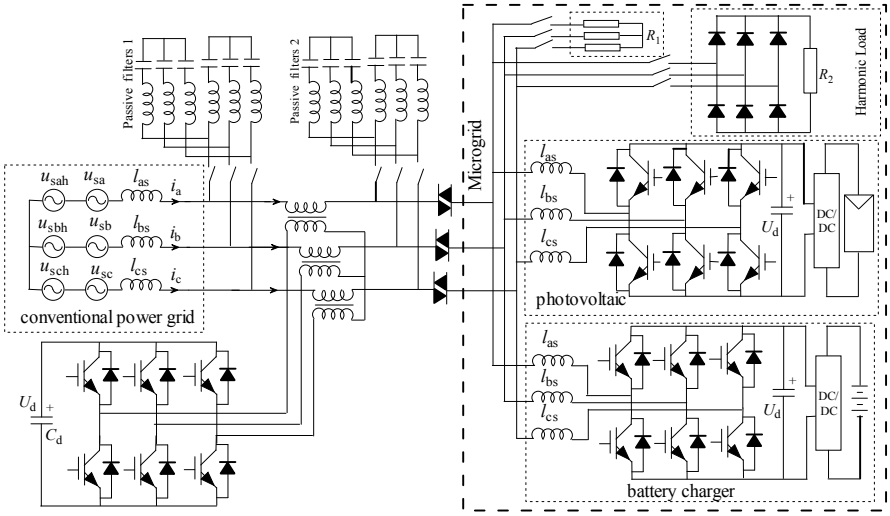

Fig.8 Circuit of the proposed integrated power quality controller

shown in Fig. 9 when the novel variable reactor is connected in series between the sending and receiving ends. Suppose the equivalent impedance Z_1+ (1-α)Z_m of the variable reactor is R+jX. In terms of the vector diagram of Fig.9, the following equations can be obtained.

$$U_m \cos\varphi = U_s \cos(\varphi - \delta) + RI \tag{21}$$

$$U_m \sin\varphi = U_s \sin(\varphi - \delta) + XI \tag{22}$$

Multiply cosφ in both sides of (21) and multiply sinφ in both sides of (22), then the following equation can be obtained by adding them.

$$U_m(U_m - U_s \cos\delta) = PR + QX \tag{23}$$

Multiply sinφ in both sides of (21) and multiply cosφ in both sides of (22), then the following equation can be obtained by subtracting them.

$$U_s \sin\delta = PX - QR \tag{24}$$

In term of (23)-(24), the active power and reactive power from U_m to U_s are

$$P = \frac{U_m}{R^2 + X^2}[R(U_m - U_s \cos\delta) + XU_s \sin\delta] \tag{25}$$

$$Q = \frac{U_m}{R^2 + X^2}[-RU_s \sin\delta + X(U_m - U_s \cos\delta)] \tag{26}$$

In the power system with high voltage level, the inductive reactance component of the transmission line is much more than the resistance component of the transmission line, (25)-(26) become

$$P = \frac{U_s U_m}{X}\sin\delta \qquad Q = \frac{U_m}{X}(U_m - U_s \cos\delta) \tag{27}$$

In microgrid with low voltage level, when the resistance component of the transmission line is much more than the inductive reactance component of the transmission line, the (25)-(26) can be expressed as

$$P = \frac{U_m}{R}(U_m - U_s \cos\delta) \qquad Q = -\frac{U_m U_s}{R}\sin\delta \tag{28}$$

In terms of (28), there is a striking difference in power flow control, voltage regulation between microgrid and conventional power grid.

C. Fault Current Limiter

When the terminal AX is connected in series in circuit, in the normal operation state, the coefficient α can be controlled as $\alpha = 1+Z_1/Z_m$, the equivalent impedance of the primary winding AX is zero. Hence, the series transformer does not have any influence on the power system normal operation. The maximum system current I_{smax} of the three phases is obtained by a current detecting circuit and compared with a reference current. In case of a short-circuit fault, maximum system current I_{smax} reaches the reference current, the coefficient α can be controlled between -1 and 1 in terms of the requirement of fault current, equivalent impedance of the primary winding AX is controlled between Z_1+Z_m and Z_1 so as to limit the system current to a desired value.

D. Voltage Compensation

In order to compensate the voltage fluctuation, the primary winding of the transformer is connected in series between the power electric utility and the load. When the load voltage is higher than the desired voltage, the coefficient α can be controlled between 0 and $1+Z_1/Z_m$, the primary winding exhibits inductive impedance. When the load voltage is lower than the desired voltage, the coefficient α is controlled more than $1+Z_1/Z_m$, the primary winding exhibits capacitive impedance. Therefore the load voltage can be controlled as a stable voltage.

E. Harmonic Isolation

The above function of power flow control, fault current limiter and voltage compensation is concerned with the fundamental. If there exits harmonic in the power utility, the primary current contains the fundamental current and nth order harmonic currents, that is to say, $i_1 = i_1^{(1)} + \Sigma\, i_1^{(n)}$. The fundamental component $i_1^{(1)}$ rather than harmonic is detected from the primary winding current i_1 and function as reference signal. A voltage source inverter is applied to track the fundamental reference signal $i_1^{(1)}$ so as to produce a fundamental compensation current $i_2^{(1)}$, which has the same

This article has been accepted for publication in a future issue of this journal, but has not been fully edited. Content may change prior to final publication. Citation information: DOI 10.1109/TIE.2014.2362495, IEEE Transactions on Industrial Electronics

frequency as $i_1^{(1)}$. $i_2^{(1)}$ is inversely in phase injected to the secondary winding *ax*. When $\alpha = 1+Z_1/Z_m$, the fundamental equivalent impedance of primary winding *AX* is zero, which is shown in Fig. 10. Meanwhile, for the nth order harmonic, since only a fundamental current is injected to the secondary winding of the transformer, i_2 does not include any order harmonic current other than the fundamental current, which means the transformer is open circuit to harmonic current. Therefore, the equivalent circuit of the transformer to the nth order harmonic is shown in Fig. 11. Then harmonic equivalent impedance of the transformer is $Z_{AX}^{(n)} = (r_1 + \mathrm{j}nx_1) + \mathrm{j}nx_m \approx nZ_m^{(1)}$. From primary winding, the series transformer exhibits very low impedance at the fundamental and simultaneously exhibits high impedance to harmonics so as to act as a "harmonic isolator". And then, the harmonic currents are forced to flow into the passive LC filter branches in both sides.

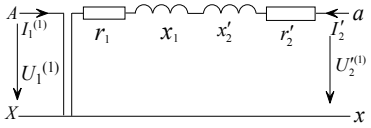

Fig.10 Fundamental equivalent circuit

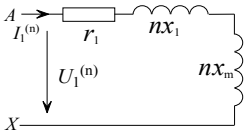

Fig.11 Harmonic equivalent circuit

F. *Integrated Power Quality Controller*

When integrating the above functions of variable reactor, power flow control, fault current limiter, voltage compensation and harmonic isolation, a novel integrated power quality controller can be achieved. For fundamental and harmonic, the primary winding of the series transformer exhibits the impedance of $Z_1^{(1)} + (1-\alpha)Z_m^{(1)}$ and $nZ_m^{(1)}$, respectively. That is to say, the primary winding of the series transformer exhibits adjustable impedance, which plays the role of power flow control, fault current limiter and voltage compensation to fundamental. Meanwhile, the primary winding of the series transformer exhibits high impedance $nZ_m^{(1)}$ to harmonic which can improves greatly the source impedance to harmonics really acts as a "harmonic isolator". Therefore, it can mitigate the harmonic high penetration.

IV. Experimental Results

To demonstrate the validity of the novel variable reactor and the integrated power quality controller for microgrid, a prototype has been constructed in terms of system schematic diagram Fig.8. Herein, the turns ratio of series transformer is 1:1, magnetizing impedance Z_m is 16.309 Ω, leakage impedance Z_1 is equal to 0.088Ω. The system voltage is 172V. The inverter switching device is FS200R12PT4 from Infineon Technologies. TMS320F28335 from Texas Instruments Inc. is applied as system microcontroller.

A. *Verification of Variable Reactor*

To begin with, the principle circuit of the variable reactor is established by simplifying the Fig.8, which is shown in Fig.12. Z_1 and Z_2 are used as experimental loads. Z_1= 3.787+j0.232Ω and Z_2=1.583+j0.097Ω. Switch K_1 always keeps with open circuit in the verification experiment of the variable reactor. The secondary winding current of the transformer is adjusted continuously. Suppose α changes between -1 and 1, the measured voltage across U_{AX} and the measured current I_1 of the primary winding is observed, so the equivalent impedance of the primary winding can be calculated accordingly. The results are shown in TABLE II. From TABLE II, the calculated equivalent Z_{AX} on the base of observation impedance is almost equal to Z_1+ (1-α) Z_m, which prove the validity of the novel principle of the transformer based on the magnetic flux controllable.

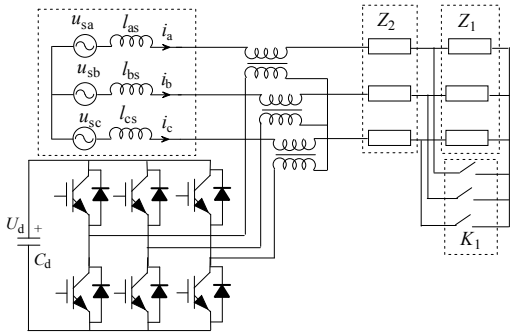

Fig.12 Principle circuit of variable reactor

TABLE II
EQUIVALENT IMPEDANCE OF THE PRIMARY WINDING WHEN α CHANGES BETWEEN -1 AND 1

α	U_{AX}(V)	I_1(A)	Z_{AX} (Ω)	Z_1+(1-α) Z_m(Ω)
α=-1	137.8	4.2	32.8095	32.706
α=-0.8	137.3	4.7	29.2127	29.4442
α=-0.6	136.4	5.2	26.2308	26.1824
α=-0.4	135.3	5.9	22.9322	22.9206
α=-0.2	133.7	6.8	19.6618	19.6588
α=0	131.3	8.0	16.4125	16.397
α=0.2	127.2	9.7	13.1134	13.1352
α=0.4	120.1	12.2	9.8443	9.8734
α=0.6	105.2	15.9	6.6163	6.6116
α=0.8	71.5	21.4	3.3411	3.3498
α=1	2.5	25.8	0.0969	0.088

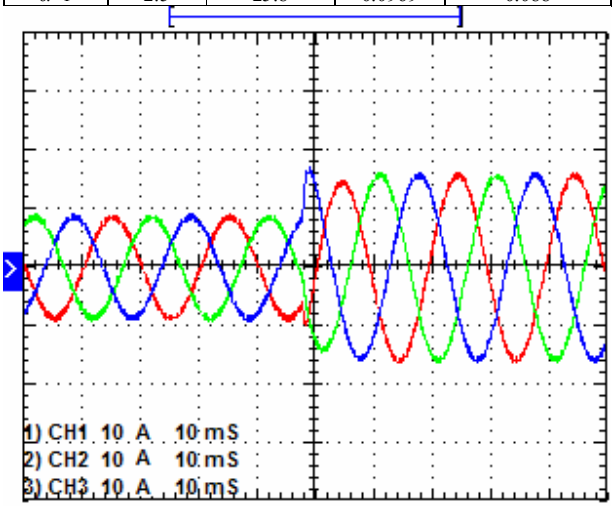

Fig.13 Current waveforms of primary winding when α suddenly changes from 0.1 to 0.6

This article has been accepted for publication in a future issue of this journal, but has not been fully edited. Content may change prior to final publication. Citation information: DOI 10.1109/TIE.2014.2362495, IEEE Transactions on Industrial Electronics

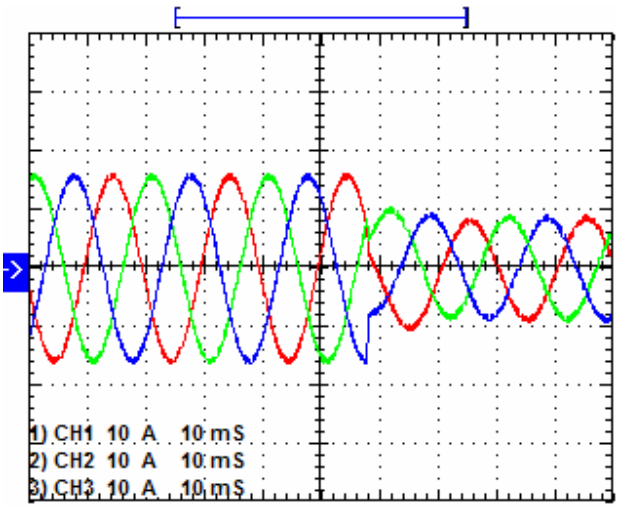

Fig.14 Current waveforms of primary winding when α suddenly changes from 0.6 to 0.1

Fig.13 and Fig.14 record the transient current waveforms of primary winding when the injected primary currents change suddenly. Fig.13 shows current waveforms of primary winding when α suddenly changes from 0.6 to 0.1. Fig.14 shows current waveforms of primary winding when α suddenly changes from 0.1 to 0.6. The above current waveforms imply the transformer with magnetic flux controllable own excellent transition characteristic. The characteristic will be very valuable in the application of FACTS controllers.

B. Verification of Fault Current limiter

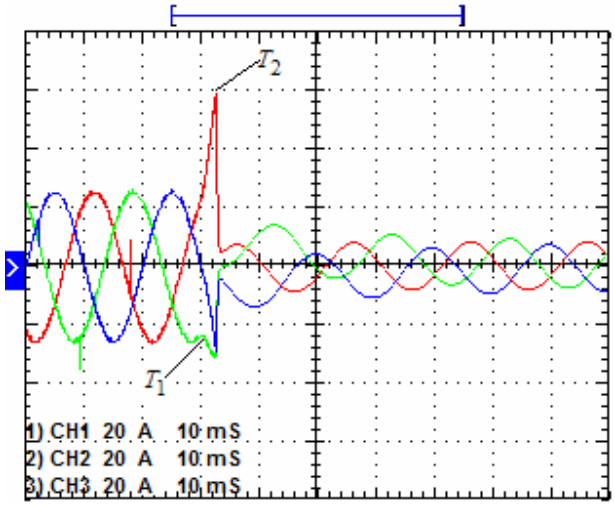

Fig.15 Current waveforms of fault current limiter.

In Fig.12, Switch K_1 is used for producing a fault. When the switch K_1 is turned on, i.e., the resistor Z_1 is short-circuited, the system current will increase greatly. A current detecting circuit is applied to obtain the maximum system current I_{smax} of the three phases. I_{smax} is used to compare with a reference current. When it reaches the reference current, the compensation coefficient α is adjusted to 0, namely, the secondary winding of the transformer is open. The primary winding exhibits the magnetizing impedance so as to limit the system current. Fig.15 shows the current waveforms of the variable reactor when it works in the condition of fault current limiter. The system current is 18.23A when the system normally operates. At time T_1, the fault happens, the system current increase rapidly. When maximum current of a certain phase reaches 60A, which is assumed to happen at time T_2, the compensation coefficient α is adjusted to 0, the system will be limited to 6.08A.

C. Verification of Harmonic High Penetration Mitigation and Filtering

In order to verify the function of the harmonic high penetration mitigation of the integrated power quality controller, the experiments are made in two conditions: 1) the voltages or currents at power supply side contain harmonics, 2) the voltages or currents at Microgrid side contain harmonics.

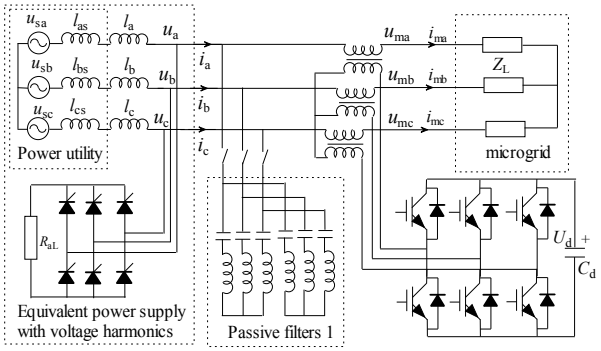

Fig.16 Experimental circuit for harmonic isolation in first condition

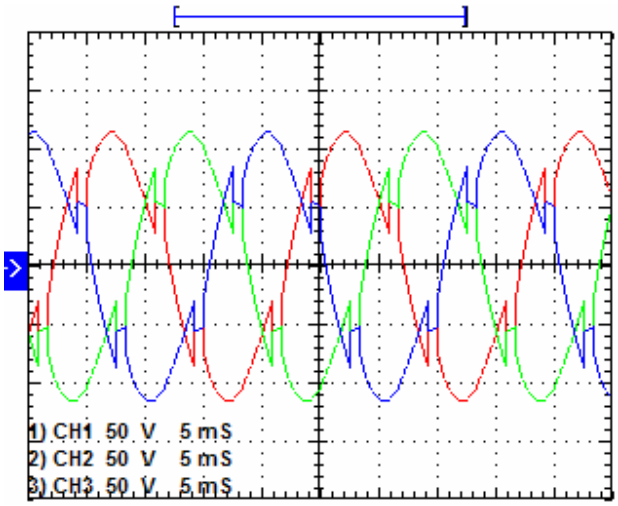

Fig.17 System voltage waveforms when the IPQC is not applied

The experimental circuit in first condition is shown in Fig.16. A three phase resistor Z_L is used to substitute the overall microgrid. A harmonic source is connected in parallel with the power system and a three-phase additional reactor indicated by l_a, l_a and l_c with the inductance of 2.51mH is connected in series with power system at power supply side in order to produce the equivalent power utility background harmonics. Figs.17 and 18 show the waveforms of the system voltages u_a, u_b and u_c and currents i_a, i_b and i_c when the integrated power quality controller and Passive filter 1 are not applied. In this case, the currents i_{ma}, i_{mb} and i_{mc} at microgrid side, namely, the system currents i_a, i_b and i_c, will also contain the same harmonic as the system current. When the integrated power quality controller and Passive filter 1 (C3=40uF, L3=28.17mH, C5=20uF, L5=20.28mH) are applied, the current waveforms of i_{ma}, i_{mb}, i_{mc}

This article has been accepted for publication in a future issue of this journal, but has not been fully edited. Content may change prior to final publication. Citation information: DOI 10.1109/TIE.2014.2362495, IEEE Transactions on Industrial Electronics

at microgrid side and the DC voltage (blue curve 4) of the capacitor C_d are shown in Fig.19. The voltage u_{ma}, u_{mb} and u_{mc} at microgrid side are similar to i_{ma}, i_{mb} and i_{mc} for resistor Z_L is linear. The DC voltage of DC capacitor (its capacitance and nominal voltage are 2200uF and 400V) is about 150V.

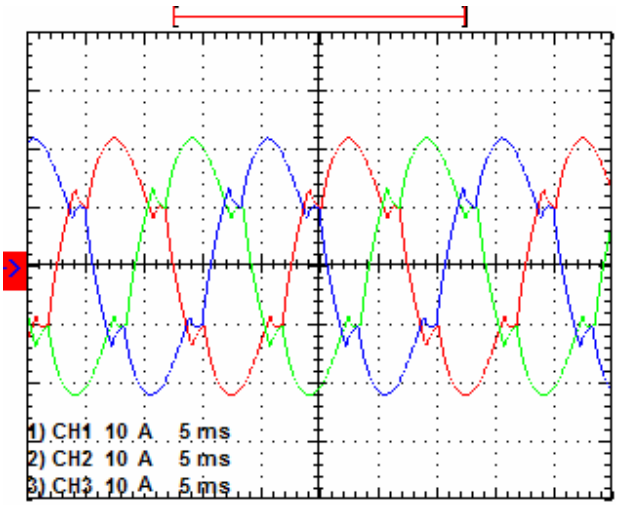

Fig.18 System current waveforms when the IPQC is not applied

In order to verify the harmonic isolation of the IPQC, the system voltage in Fig.17, the system current in Fig.18 and the current i_{ma} at microgrid side in Fig.19 of phase-*a* are analyzed into Fourier series and the results are shown in TABLE III. The THD of the system voltage and current are 16.77% and 14.74%, respectively. The THD of the current i_{ma} is 0.97%.

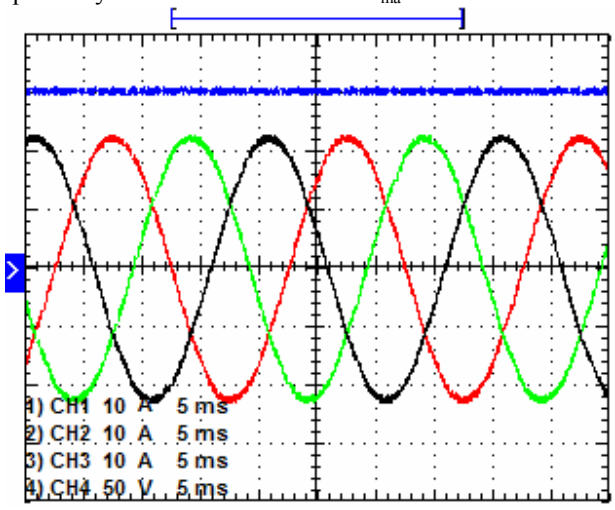

Fig.19 Current waveforms at microgrid side when the IPQC is applied

The experimental circuit in second condition is shown in Fig.20. A harmonic-producing load is used to substitute the overall microgrid. In this case, the system voltage is approximately sinusoidal. Figs.21 and 22 show the system voltage and current waveforms when the IPQC and Passive filter 2 are not employed. When the integrated power quality controller and Passive filter 2 (C3=40uF, L3=28.17mH, C5=20uF, L5=20.28mH) are employed, the system currents i_a, i_b and i_c waveforms at power utility side are shown in Fig.23. Likewise, the system voltage in Fig.21, the system current in Fig.22 and the system current in Fig.23 of phase-*a* are analyzed into Fourier series and the results are shown in TABLE IV. The THD of the system voltage and current when the IPQC and Passive filter 2 are employed are 2.92% and 41.06%, respectively. The THD of System current i_a at power utility side is 1.17% when the IPQC and Passive filter 2 are employed.

TABLE III
MAIN HARMONIC CONTENTS OF EXPERIMENTAL RESULTS IN FIRST CONDITION

Harmonic orders	System Voltage (V)	system current (A)	the currents i_{ma} at microgrid (A)
1	106.4383	20.7364	21.1233
3	0.0248	0.002	0.0001
5	14.095	2.5157	0.0183
7	9.2985	1.552	0.1604
9	0.0527	0.0002	0.0001
11	5.1521	0.7254	0.1019
13	3.8142	0.5009	0.07
15	0.0337	0.0002	0.0001
17	0.685	0.0801	0.0237
19	0.252	0.0273	0.0173
21	0.0152	0.0001	0
23	1.6178	0.1344	0.0108
25	1.6662	0.1344	0.0095
THD	16.77%	14.74%	0.97%

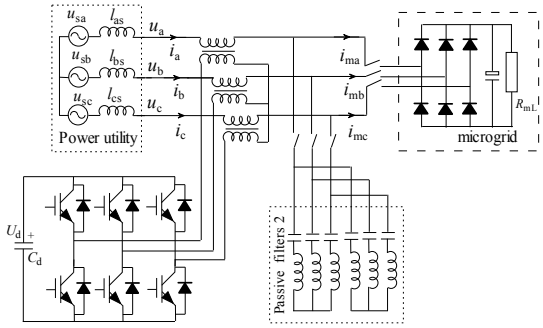

Fig.20 Experimental circuit for harmonic isolation in second condition

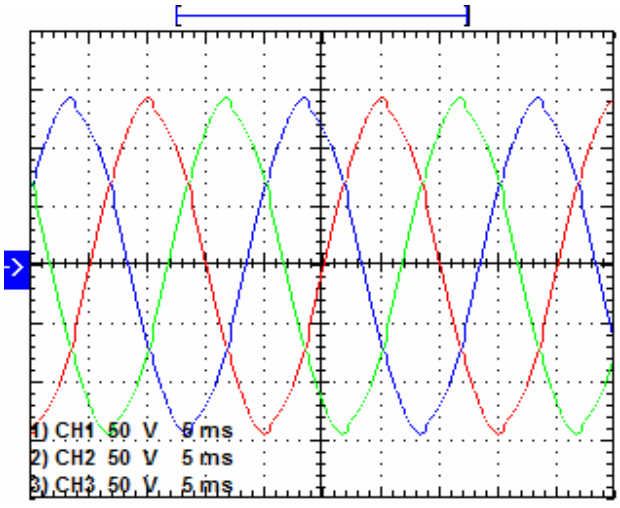

Fig.21 System voltage waveforms when the IPQC is not employed

In terms of the experimental results in two conditions, the IPQC plays the role of isolating harmonic. It can isolate both the harmonic from the power utility and the harmonic from microgrid. The harmonic currents are forced to flow into the passive LC filter branches in both sides. Therefore, the novel IPQC can mitigate the harmonic high penetration.

This article has been accepted for publication in a future issue of this journal, but has not been fully edited. Content may change prior to final publication. Citation information: DOI 10.1109/TIE.2014.2362495, IEEE Transactions on Industrial Electronics

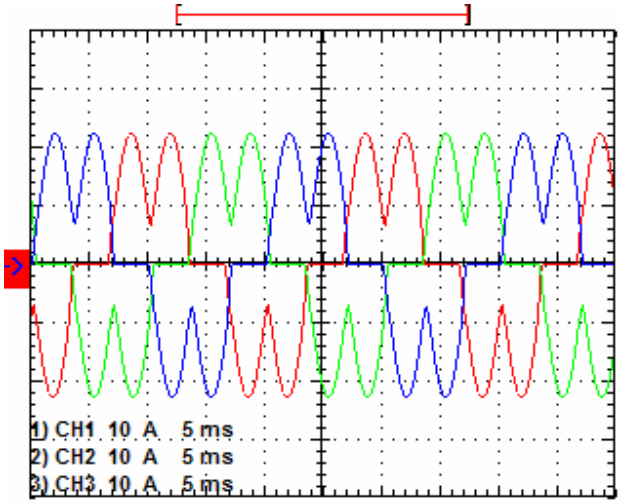

Fig.22 System current waveforms when the IPQC is not employed

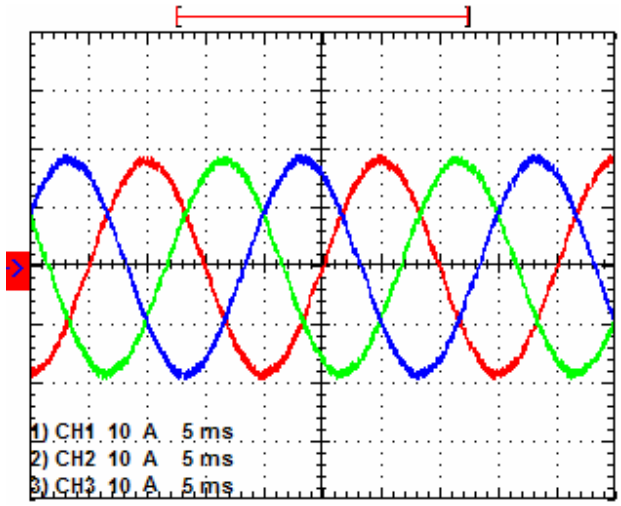

Fig.23 System current waveforms when the IPQC is employed

TABLE IV
MAIN HARMONIC CONTENTS OF EXPERIMENTAL RESULTS IN SECOND CONDITION

Harmonic orders	System voltage (V)	System current (A) when IPQC is not applied	System current (A) when IPQC is not applied
1	139.4	18.4491	18.3577
3	0.0005	0.02	0.0052
5	3.4892	7.2418	0.0235
7	1.0923	1.6774	0.1342
9	0.0003	0.0239	0.0044
11	1.312	1.2648	0.1314
13	0.3573	0.2537	0.0862
15	0.0001	0.0363	0.0019
17	0.8593	0.5467	0.0277
19	0.3312	0.2193	0.0291
21	0.0001	0.0335	0.0012
23	0.6242	0.291	0.0243
25	0.3611	0.1316	0.0169
THD	2.92%	41.06%	1.17%

V. CONCLUSION

The paper presents a novel variable reactor based on the magnetic flux control. A transformer with air gap is selected and the primary winding current of the transformer is detected. A voltage-sourced inverter is applied to follow the primary current so as to produce another current, which is injected to the secondary. When the injected current is adjusted, the equivalent impedance of primary winding of the transformer will change continuously. The variable reactor features hardly producing harmonics, simple control scenario and with consecutive adjustable impedance. The ramp comparison current control with PI controller, which is suitable for DSP microcontroller, is chosen as control current. The optimum PI controller parameters choosing criteria is given in this paper. When the injected current varies suddenly, the novel variable reactor has excellent dynamic characteristic.

In terms of the novel variable reactor, a novel integrated power quality controller suitable for microgrid is proposed. The primary winding exhibits adjustable impedance, which plays the role of power flow control, fault current limiter and voltage compensation to fundamental. Meanwhile the primary winding exhibits high impedance to harmonic which can improves greatly the source impedance to harmonics really acts as a "harmonic isolator". Therefore, it can mitigate the harmonic high penetration.

A set of three-phase integrated power quality controller has been constructed. The experimental test results verify the validity of the novel variable reactor and the integrated power quality controller.

REFERENCES

[1] B. Lasseter, "Microgrids [distributed power generation]," *IEEE Power Engineering Society Winter Meeting*, Vol.1, pp. 146-149, 2001

[2] C. Marnay, F.J. Robio, A.S. Siddiqui, "Shape of the microgrid," *IEEE Power Engineering Society Winter Meeting*, 2001. Vol.1, pp. 150-153, 2001

[3] R. H. Lasseter, A. Akhil, C. Marnay, et al. "Integration of distributed energy resources: the CERTS microgrid concept," *USA: Consortium for Electric Reliability Technology Solutions*, 2002.

[4] C. Marnay, O. Bailey, "The CERTS Microgrid and the Future of the Macrogrid," *LBNL-55281*. August 2004

[5] N. Hatziargyriou, H. Asano, R. Iravani, C. Marnay, "Microgrids," *IEEE Power and Energy Magazine*, vol.5, no.4, pp. 78-94, July/Aug. 2007

[6] R. H. Lasseter, "Smart Distribution: Coupled Microgrids," *Proceedings of the IEEE*, vol.99, no.6, pp. 1074-1082, 2011

[7] H. Akagi, E. H. Watanabe, M. Aredes, *Instantaneous Power Theory and Applications to Power Conditioning*, IEEE Press, 2007, pp. 1-17

[8] C. Sankaran. *Power quality*. Boca Raton : CRC Press, 2002, pp. 133-146

[9] R. C. Dugan, *Electrical power systems quality*, New York : McGraw-Hill, 2003, pp. 167-223

[10] A. Baggini, Handbook of Power Quality, John Wiley & Sons Inc., 2008, pp. 187-257

[11] B. Singh, K. Al-Haddad, A. Chandra, "A Review of active filters for power quality improvement," *IEEE Trans. Ind. Electron.*,vol.46, no.5, pp. 960-971, Oct. 1999

[12] F. Z. Peng, "Application issues of active power filters," *IEEE Industry Application Magazine*, 21-30, Sep./Oct. 1998

[13] K. M. Smedley, L. Zhou, C. Qiao. "Unified constant-frequency integration control of active power filters – steady-state and dynamics," *IEEE Trans. Power Electron.*, vol.16, no.3, pp. 428-436, May 2001.

[14] H. Rudnick, J. Dixon, L. Moran, "Delivering clean and pure power," *IEEE Power and Energy Magazine*, Vol.1, pp. 32-40, Sep./Oct. 2003

[15] S. Buso, L. Malesani, P. Mattavelli, "Comparison of current control techniques for active filter applications," *IEEE Trans. Ind. Electron.,* Vol. 45, pp. 722-729, Oct. 1998.

[16] M. Aredes, J. Hafner, K. Heumann, "Three-phase four-wire shunt active filter control strategies," *IEEE Trans. Power Electron.*, vol.12, 311–318, Mar. 1997.

[17] J. He, Y. W. Li, D. Bosnjak, B. Harris "Investigation and active damping of multiple resonances in a parallel-inverter-based microgrid," *IEEE Trans. Power Electron.*, vol.28, no.1, pp.234-246, Jan. 2013

This article has been accepted for publication in a future issue of this journal, but has not been fully edited. Content may change prior to final publication. Citation information: DOI 10.1109/TIE.2014.2362495, IEEE Transactions on Industrial Electronics

[18] J. M. Guerrero, P. C. Loh, T. -L. Lee, M. Chandorkar, "Advanced control architectures for intelligent microgrids-part II: power quality, energy storage, and AC/DC microgrids," *IEEE Trans. Ind. Electron.*, vol.60, no.4, pp. 1263-1270, Apr. 2013

[19] J. He, Y. Li, F. Blaabjerg, "Flexible Microgrid Power Quality Enhancement Using Adaptive Hybrid Voltage and Current Controller," *IEEE Trans. Ind. Electron.*, vol.61, no.6, pp: 2784-2794, June 2014.

[20] Y. Li, M. Vilathgamuwa, P. C. Loh, "Microgrid power quality enhancement using a three-phase four-wire grid-interfacing compensator," *IEEE Trans. Ind. Appl.,* vol. 41, no.6, pp. 1707-1719, Nov/Dec 2005

[21] D. Menniti, A. Burgio, A. Pinnarelli, N. Sorrentino, "Grid-interfacing active power filters to improve the power quality in a microgrid," *13th International Conference on Harmonics and Quality of Power*, pp. 1-6, 2008

[22] F. Blaabjerg, R. Teodorescu, M. Liserre, A.V. Timbus, "Overview of Control and Grid Synchronization for Distributed Power Generation Systems," *IEEE Trans. Ind. Electron.*, vol. 53, no. 5, pp. 1398-1409, Oct 2006.

[23] J.M. Guerrero, J.C. Vasquez, J. Matas, L.G. de Vicuna, M. Castilla, "Hierarchical Control of Droop-Controlled AC and DC Microgrids—A General Approach Toward Standardization," *IEEE Trans. Ind. Electron.*, vol. 58, no. 1, pp. 158 - 172 , Jan 2011.

[24] R. Majumder, A. Ghosh, G. Ledwich, and F. Zare, "Power management and power flow control with back-to-back converters in a utility connected microgrid," *IEEE Trans. Power Syst.*, vol. 25, no. 2, pp. 821–834, May 2010.

[25] X. Yu, A. M. Khambadkone, H. Wang, and S. T. S. Terence, "Control of parallel-connected power converters for low-voltage microgrid—Part I: A hybrid control architecture," *IEEE Trans. Power Electron.*, vol. 25, no. 12, pp. 2962–2970, Dec. 2010.

[26] M. Prodanovic, T. C. Green, "High-quality power generation through distributed control of a power park microgrid," *IEEE Trans. Ind. Electron.*, vol.53, no.5, pp. 1471-1482, 2006

[27] F. Wang, J. L. Duarte, M. A. M. Hendrix, "Grid-interfacing converter systems with enhanced voltage quality for microgrid application—concept and implementation," *IEEE Trans. Power Electron.*, vol.26, no.12, pp. 3501-3513, 2011

[28] M. Savaghebi, A. Jalilian, J. C. Vasquez, J. M. Guerrero, "Autonomous voltage unbalance compensation in an islanded droop-controlled microgrid," *IEEE Trans. Ind. Electron.*, vol.60, no.4, pp.1390-1402, 2013

[29] T. -L. Lee; S. –H. Hu; Y. –H. Chan. "D-STATCOM with positive-sequence admittance and negative-sequence conductance to mitigate voltage fluctuations in high-level penetration of distributed-generation systems," *IEEE Trans. Ind. Electron.*, vol.60, no.4, pp. 1417 – 1428, Apr. 2013

[30] R. Majumder, "Reactive power compensation in single-phase operation of microgrid," *IEEE Trans. Ind. Electron.*, vol. 60, no.4, pp. 1403 – 1416, April 2013

[31] M. Azizi, A. Fatemi, M. Mohamadian, A.Y.Varjani, "Integrated solution for microgrid power quality assurance," *IEEE Transactions on Energy Conversion*, vol.27, no.4, pp. 992-1001, 2012

[32] H. J. Laaksonen, "Protection principles for future microgrids," *IEEE Trans. Power Electron.*, vol.25, no.12, pp. 2910-2918, 2010

[33] T. Ghanbari, E. Farjah, "Unidirectional fault current limiter: an efficient interface between the microgrid and main network," *IEEE Trans. Power Systems*, vol.28, no.2, pp. 1591-1598, 2013

[34] A. H. Etemadi, R. Iravani, "Overcurrent and overload protection of directly voltage-controlled distributed resources in a microgrid," *IEEE Trans. Ind. Electron.*, vol. 60, no. 12, pp. 5629-5638, Dec 2013.

[35] T. –F. Wu, H. –S. Nien, C. –L. Shen, T. –M. Chen . "A single-phase inverter system for PV power injection and active power filtering with nonlinear inductor consideration," *IEEE Trans Ind. Appl.*, vol.41, no.4, pp. 1075-1084, 2005

[36] A. E. Fitzgerald, Charles Kingsley, Jr., Stephen D. Umans, *Electric Machinery*, McGraw-Hill Higher Education, 2003. pp. 57-81

[37] Paul C. Krause, Oleg Wasynczuk, Scott D. Sudhoff, *Analysis of electric machinery and drive systems*, John Wiley & Sons, Inc, pp. 1-11, 2002

[38] N. G. Hingorani, L. Gyugyi, *Understanding FACTS: Concepts and Technology of Flexible AC Transmission Systems*, IEEE Press, 2000, pp. 1-29

[39] Seung-Ki Sul, *Control of Electric Machine Drive Systems*, John Wiley & Sons, Inc, pp. 154-215, 2011

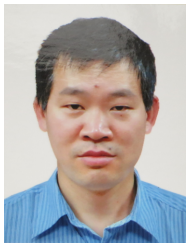

Dayi Li (M'12) received the B.S. degree from Tianjin Polytechnic University in 1995, and M.S. and Ph.D. degrees from Huazhong University of Science and Technology (HUST) in 2000 and 2005, respectively. From 1995 to 1997, he was an Electrical Engineer at Wuhan No.3 Cotton Mill Company. In 2000, he joined HUST as Assistant Professor and currently is Associate Professor. From 2011 to 2012, he was a visiting researcher in the Department of Electronic and Electrical Engineering at the University of Sheffield, UK. His research interests are power quality controller, transformer and power electronics.

Z. Q. Zhu(M'90–SM'00–F'09) received the B.Eng. and M.Sc. degrees in electrical and electronic engineering from Zhejiang University, Hangzhou, China, in 1982 and 1984, respectively, and the Ph.D.degree in electrical and electronic engineering from the University of Sheffield, Sheffield, U.K., in 1991. He is currently Professor of electrical machines and control systems at the University of Sheffield, Head of the Electrical Machines and Drives Research Group, and Academic Director of Sheffield Siemens Wind Power Research Centre. His major research interests include design and control of permanent magnet brushless machines and drives, for applications ranging from automotive engineering to renewable energy.